Status of the K2K thin target analysis

J.J Gomez-Cadenas*

November 25, 2004

Abstract

In this note the status of the measurement of the cross section of protons on thin Al target at 12.9 GeV –K2K thin Al target analysis– is presented.

1 Introduction

HARP (Fig. 1) is a large acceptance spectrometer, with two distinct regions. In the forward part of the apparatus (up to polar angles of about 250 $mrad$), the main tracking devices are a set of large drift chambers, reused from the NOMAD experiment (modules NDC1 to NDC5). Magnetic analysis is provided by a 0.4 T dipole magnet and particle identification relies in the combination of a threshold Cherenkov detector (CHE), a time-of-flight wall (TOF) and an electromagnetic calorimeter. In the rest of the solid angle the main tracking device is a TPC, which is complemented by a set of RPC detectors for time-of-flight measurements. The target is located inside the TPC. In addition, sophisticated beam instrumentation (including three timing detectors and threshold Cherenkov detectors) provides identification of the incoming particle and allows the interaction time at the target to be measured.

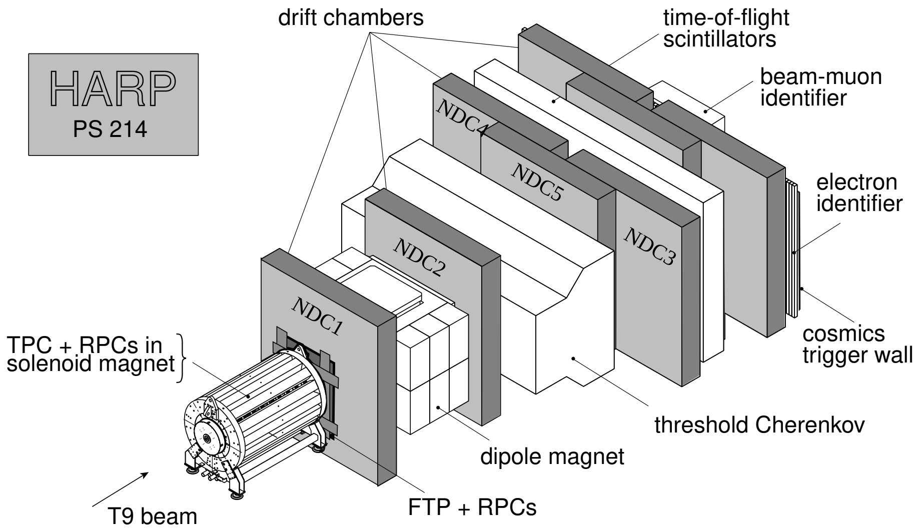

Figure 1: Schematic layout of the HARP spectrometer.

The goal of this analysis is to measure the cross section of protons of 12.9 GeV impinging in a thin Al target, using the forward part of the HARP spectrometer. This measurement is useful as imput for the calculation of the Far/Near ratio in the K2K experiment.

*On behalf of the HARP analysis group

The K2K neutrino beam is originated by the decay of hadrons produced in 12.9 GeV proton-Al collisions. The pion yield in K2K is measured for momentum above 2 GeV/c–which corresponds to neutrino energies roughly about 1 GeV– using a Cherenkov detector with variable refraction index, called PIMON. For pion momenta below 2 GeV/c, the calculation of the flux has to rely on a the extrapolation of a parameterization that describes well the data on the region covered by PIMON.

Consequently, the data critical for K2K is pion yields at low momentum. Harp acceptance is such that pions can be measured with good efficiency for momenta above 1 GeV/c. A measurement of the cross section between 1 and 6 GeV/c would be sufficient to, a) cover the critical region where oscillations effects are maximal and there is no PIMON data –between pion momenta of 1 to 2 GeV/c, corresponding to neutrino energies of 0.5 to 1 GeV–, and b) permit matching with PIMON data –between pion momenta of 2 to 6 GeV/c– which ensures consistency of both measurements.

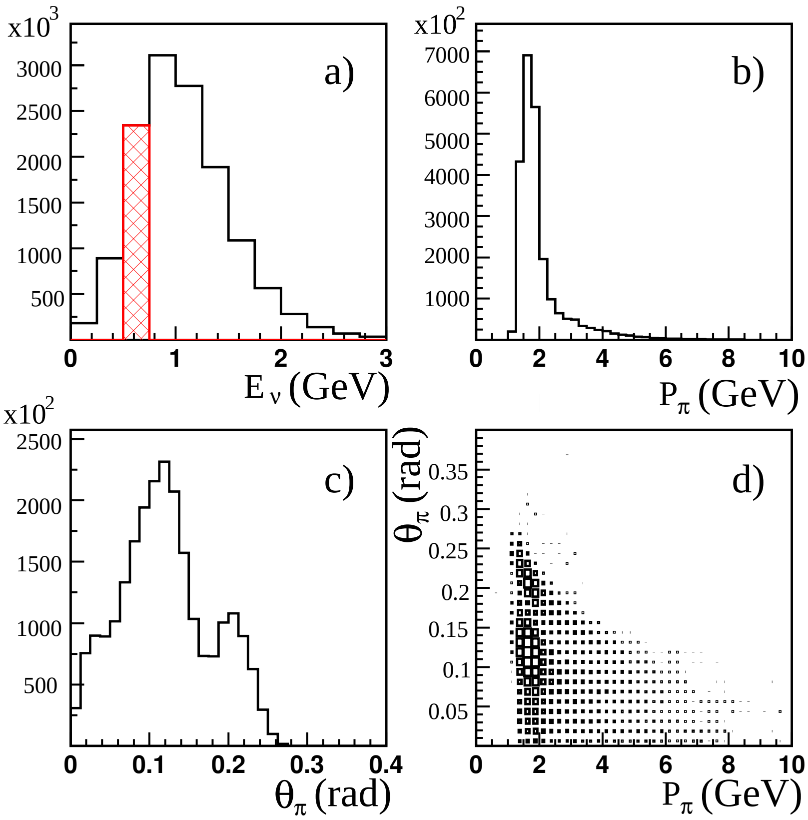

Figure 2: a) Neutrino interaction spectrum at the K2K near detector. The peak of the oscillation correspond to the hatched bin. b) Momentum distribution of pions producing neutrinos with energies in the range 0.5-0.75 GeV/c. c) Angular distribution for the selected pions. d) Angle versus momentum for the selected pions.This plot,courtesy of the K2K collaboration

Fig. 2 (upper-left) shows a Monte Carlo simulation of the interacting neutrino spectrum at the K2K near detector assuming no oscillations. The experiment is very sensitive to variations of the predicted non-oscillated spectrum in the energy range between 0.5 and about 1 GeV/c, where the deformation of the spectrum due to the atmospheric oscillation is predicted to be maximal. Also shown in 2 is the pion production cross section corresponding to pions that result in neutrinos in the energy bin (0.5-0.75 GeV/c), where the oscillation is expected to peak (shaded bin in upper-left plot), according to the K2K Monte Carlo. Right-upper plot shows the momentum distribution, lower-left plot the angular distribution (in terms of the pion momentum and polar angle, e.g, the angle with respect to the proton axis) and bottom-right the correlated p-θ distribution. Notice that the relevant angular region is below 250 mrad, while the relevant momentum region is between 1 GeV/c and is essentially exhausted at 6 GeV/c. On the other hand, the distribution is strongly peaked at 2 GeV/c, so that already at 3 GeV/c one is essentially measuring a small tail.

The momentum and angular range relevant for the K2K calculation is very well matched by HARP momentum and angular acceptance. In addition, particle identification is very good in the whole relevant momentum range thanks to the combination of TOF, CHE and ECAL.

Tracking in HARP is challenging due to low hit-efficiency, related with the non-flamable gas mixture used by the NDCs. In addition, the chambers near to the target suffer from saturation (due to high particle density) near the beam spot. Furthermore, every detector composing the spectrometer must be correctly aligned.

To adress the problem of low hit efficiency, we have developed a sophisticated tracking algorithm that builds three-dimensional ($3D$) segments in the NDC modules. These are later connected, using a extrapolator based on the well known mathematical technique of Kalman Filter, which provides a robust and elegant way to handle multiple scattering and energy loss. In addition, a very refined alignment procedure has been completed. Finally, the redundancy of tracking modules in HARP permits the measurement of tracking efficiency from the data themselves, thus avoiding biases asociated with insuficiently good description of our detector in the Monte Carlo simulation as well as biases associated with the hadronic model(s) used by the simulation.

PID at low momenta (up to 3-4 GeV/c) is excellent, thanks to high resolution TOF detectors (TOF beam detectors, with a resolution of about 70 ps and the TOF wall with a resolution of near 150 ps). The CHE, on the other hand, is already almost fully efficient for pion detection in the region where the TOF starts to loose sensitivity, thus guaranteing a smooth PID in the whole relevant range. Electron identification at low momenta is provided by the combination of CHE and ECAL. The rare electrons present at high momenta are easily supressed by ECAL.

This note is organized as follows. Tracking in HARP is reviewed in section 2. In section 3 we discuss the ingredients that enter into the calculation of the cross section, namely: geometrical acceptance (section 4), tracking efficiency (section 5) and PID (section 6). Finally, 7 summarizes the status of the analysis.

2 Tracking with HARP forward spectrometer

The main tracking device of the forward spectrometer is a set of drift chambers placed upstream and downstream of the dipole magnet. These chambers were recuperated from the NOMAD experiment, where they served both as a target for neutrino interactions and as a tracker for the produced charged particles. In HARP they were filled with a less efficient but non-flammable gas mixture than in NOMAD : Ar(90%)-CO_2(9%)-CH_4(1%), sense wires held at +1300V and potential wires at -2900V).

2.1 Alignment

To extract the performances of the chambers (spatial resolution and hit efficiency) an alignment of all wires had to be done first. To this extent we have used seveal track samples, namely: a) cosmic-ray events stored in between PS spills, as well as beam via a special trigger, b) beam particles with magnetic field off, c) tracks emanating from p-target collisions and d) elastic events. The alignment procedure is very involved, since one has to align each one of the NDC modules relative to the others, as well as to the PID detectors (Cherenkov, TOF and electromagnetic calorimeter), the TPC and the Beam detectors. In total more than 15000 parameters have to be adjusted iteratively. After all corrections and iterations, the resulting residual distribution is shown in Fig. 3 and gives a spatial resolution of about 340 μm. This value is about twice worse than what has been measured in the NOMAD conditions. The gas mixture can be invoked here: the longitudinal dispersion of the drifting electrons and the much reduced size of the plateau in the drift velocity distribution as a function of the electric field, both contribute to degrading the resolution. However, one should stress that this spatial resolution is more than sufficient for HARP physics.

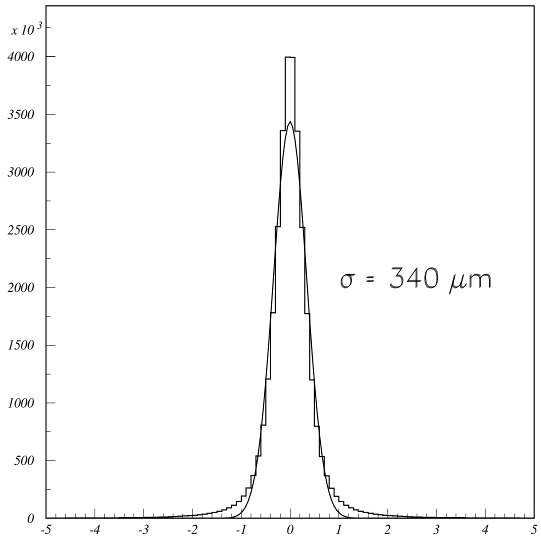

Figure 3: Residuals for a sample of cosmic-ray tracks in the drift chambers.

2.2 Hit efficiency

Hit efficiency has been computed also using several samples of data. Cosmic rays, beam particles (crossing an empty, thin, or thick target) and tracks emanating from an interaction, using the redundancy of NDC modules.

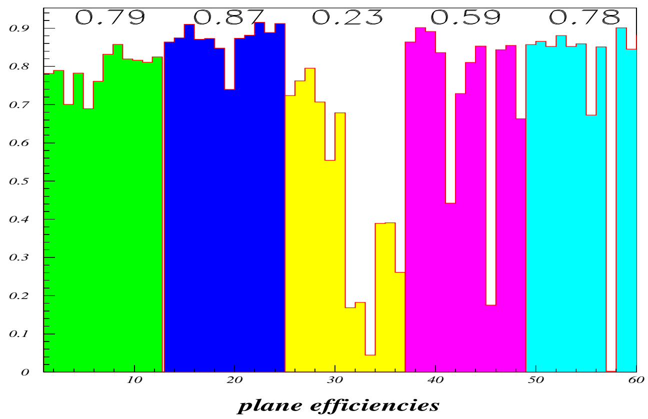

Figure 4: Hit efficiencies of the drift chamber planes, as measured from cosmic-ray data, module by module. Each module is represented with a different color (grey shade). Notice that modules 3 and 4, which have low efficiency are the side modules (see Fig. 1) outside the main fiducial volume.

Fig. 4 shows hit efficiencies per measurement plane computed with a large sample of cosmic-ray tracks. The numeration of the modules correspond to the labels in Fig. 1). The average value of the hit efficiency for the central modules lie between 80% and 85%, much lower than the NOMAD conditions (> 95%): this loss of performance can again be attributed to the change of the gas mixture and new electronics.

The reduced efficiencies of the two side modules however reflect more a specific degradation with time of chambers which have not been used for about two years (between the NOMAD and HARP data-taking periods).

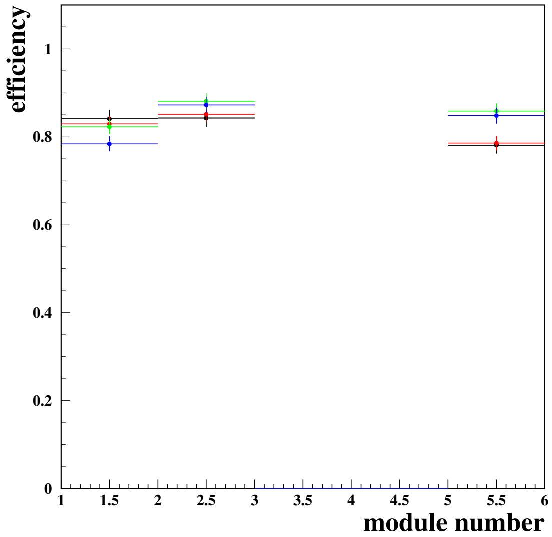

Figure 5: Average hit efficiency per module for 3, 5, 8 and 12 GeV/c thick tantalum data.

Fig. 5 shows the hit efficiency for beam particles when a thick target of about one nuclear interaction length is used. As it can be seen one obtains figures in the vicinity of 80%, consistent with the measurement using cosmic-ray data. Instead, the hit efficiency in module one decreases dramatically if measured with a thin or empty target, as shown in Fig. 6. This is related with chamber saturation due to the high intensity of the beam, as demonstrated by the fact that the efficiency decreases progressively during a spill for no target data (indicating the gradual saturation of the chamber) while remaining constant for thick target data. The efficiency is close to the nominal value at the beginning of the spill, indicating that the chambers recover between spills.

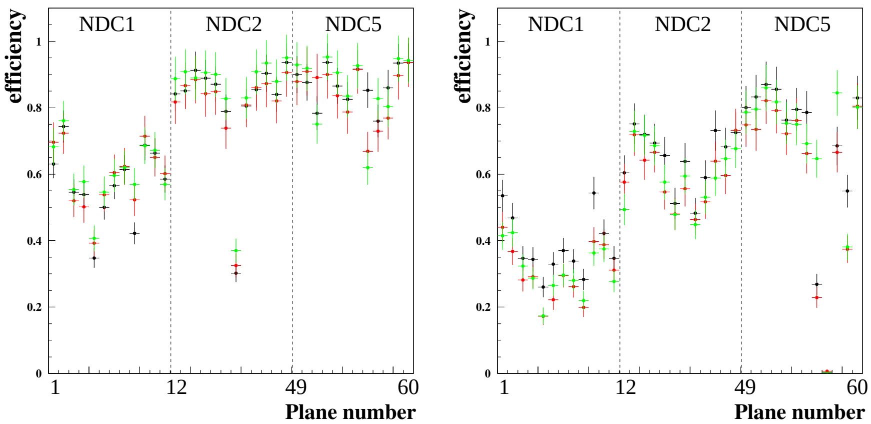

Figure 6: Hit efficiency per plane in modules 1, 2 and 5 for 3 GeV/c (left) and 15 GeV/c (right) empty target data and for 3 different run periods. The efficiency map is similar for thin target.

2.3 The segment algorithm

Reconstruction of tracks and momentum measurement in HARP's forward region is made difficult by the low efficiency of the chambers ($\sim$ 80%), which prevents a simple approach, such as the one used by the NOMAD experiment,where space points (constructed from a set of three consecutive planes at tilted angles, $-5, 0$, and 5^0 respectively) were used as the basic building block of the track reconstruction algorithm. Such an algorithm is not viable in HARP, since the efficiency to build a space-point is of the order of $80^3 \sim 50\%$.

Instead, the tracking algorithm in HARP builds three dimensional track segments in each tracking module, with an efficiency larger than 90%. Then, the isolated track segments are combined to form tracks.

Our segment algorithm builds $2D$ plane segments per module and then combines them to create $3D$ track segments (also per module). The requirements are the following:

- **Plane ($2D$) segment**: At least 3 hits in the same projection (u, x or v) compatible with being aligned. The drift sign associated to each hit is decided during the plane segment reconstruction phase.

- **Track ($3D$) segment**: Two or three plane segments of different projections, whose intersection defines a 3D straight line. In the case of two plane segments it is also required a hit in the remaining projection compatible with being intersected by the 3D straight line defined by the other two projections.

Consequently, to form a track segment at least seven hits are needed (one per plane) within the same module. The efficiency achieved by this algorithm is of the order of 90%, as shown in Fig. 7. This figure also shows a good agreement between reconstructed data and Monte Carlo simulation.

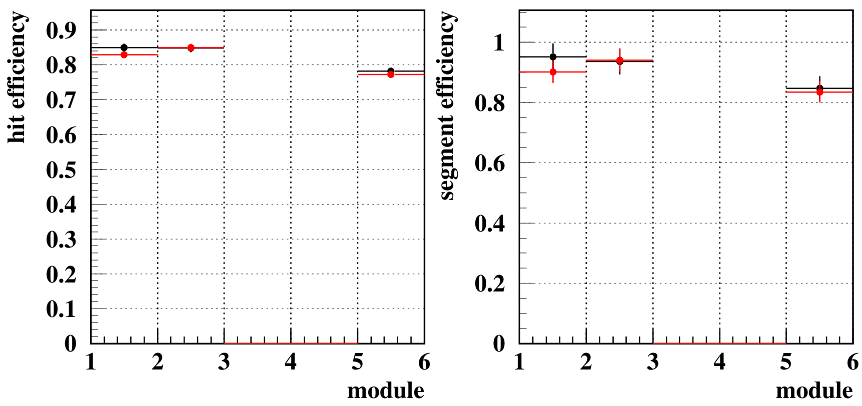

Figure 7: Hit and track segment reconstruction efficiency for 3 GeV/c empty target real data and Monte Carlo simulated data. The hit efficiency per plane of the data has been introduced in the Monte Carlo simulation.

3 Cross section

The inclusive, single-particle, pion production differential cross section can be computed as follows:

$$\sigma_i^\pi = N_{norm} \frac{1}{\varepsilon_i^{acc}} \frac{1}{\varepsilon_i^{track-eff}} \left[M_{ij} \frac{1}{\varepsilon_j^{-\pi}} \eta_j^{-\pi} \cdot N_j^{-\pi} \right] \quad (1)$$

where the indices i and j correspond to true and reconstructed (p, θ) bins respectively. ε_i^{acc} is the geometrical acceptance, $\varepsilon_i^{track-eff}$ is the tracking efficiency, M_{ij} is the migration matrix from reconstructed bin j to true bin i, ε_j^π is the pion identification efficiency, η_j^π is the pion purity and N_j^π observed particle yield. The pion purity is defined as $\eta_j^\pi = N_j^{true-\pi}/N_j^\pi = (N_j^\pi - N_j^{bkg})/N_j^\pi$, where $N_j^{true-\pi}$ is the number of true observed pions in the bin j, and N_j^{bkg} is the number of particles misidentified as pions in the same bin j. That means that η_j^π is just the probability of correct identification of a pion. The pion identification efficiency, ε_j^π is the fraction of times that a tracked pion is identified as such.

Let us now consider each term separately.

4 Acceptance

The geometrical acceptance $\varepsilon_{i\alpha}^{acc}$ of the spectrometer is defined as the ratio between the true particle yield $N_{i\alpha}$ and the yield accepted by the dipole $N_{i\alpha}^{acc}$, where the index i runs over bins of true momentum and production angle, and the index α refers to the particle type (pion, electron, etc). This index is necessary beacuse the acceptance is, a priory, different for different particle types (consider for example electron bremsstrhalung).

The geometrical acceptance can be computed with the Monte Carlo,provided that the description of the apparatus geometry and the dipole magnetic field map are accurate.

Fig. 8 shows the (pion) acceptance in bins of momentum (left) θ_x (center) and θ_y (right), where θ_x and θ_y are the cartesian components of the production angle θ. Given the dipole dimensions, the acceptance in θ_y is rather small, about 50 mrad. However, given the azimuthal symmetry of the cross-section this is not a problem. Fig. 9 shows the acceptance in bins of momentum (left) and θ_x (right) when a cut on $|\theta_y| < 50mrad$ is imposed. Since momentum and angle are correlated, Fig. 10 shows the acceptance in bins of momentum (left) when cuts on $|\theta_y| < 50mrad$, $|\theta_x| < 200mrad$ are imposed and the acceptance in bins of θ_x (right) when cuts on $|\theta_y| < 50mrad$ and $P > 1GeV$ are imposed.

Notice that both the momentum and angle acceptance are well matched to the requirements of K2K.

5 Tracking efficiency

5.1 Tracking modules

The tracking modules relevant for the analysis are shown in Fig. 11. The central modules are NDC1, NDC2 and NDC5. NDC3 and NDC4 allow extended acceptance. This is illustrated in Fig. 12.

5.2 Tracking redundancy for efficiency calculations

Tracking redundancy can be used to compute hit, segment and tracking efficiency using the data themselves.

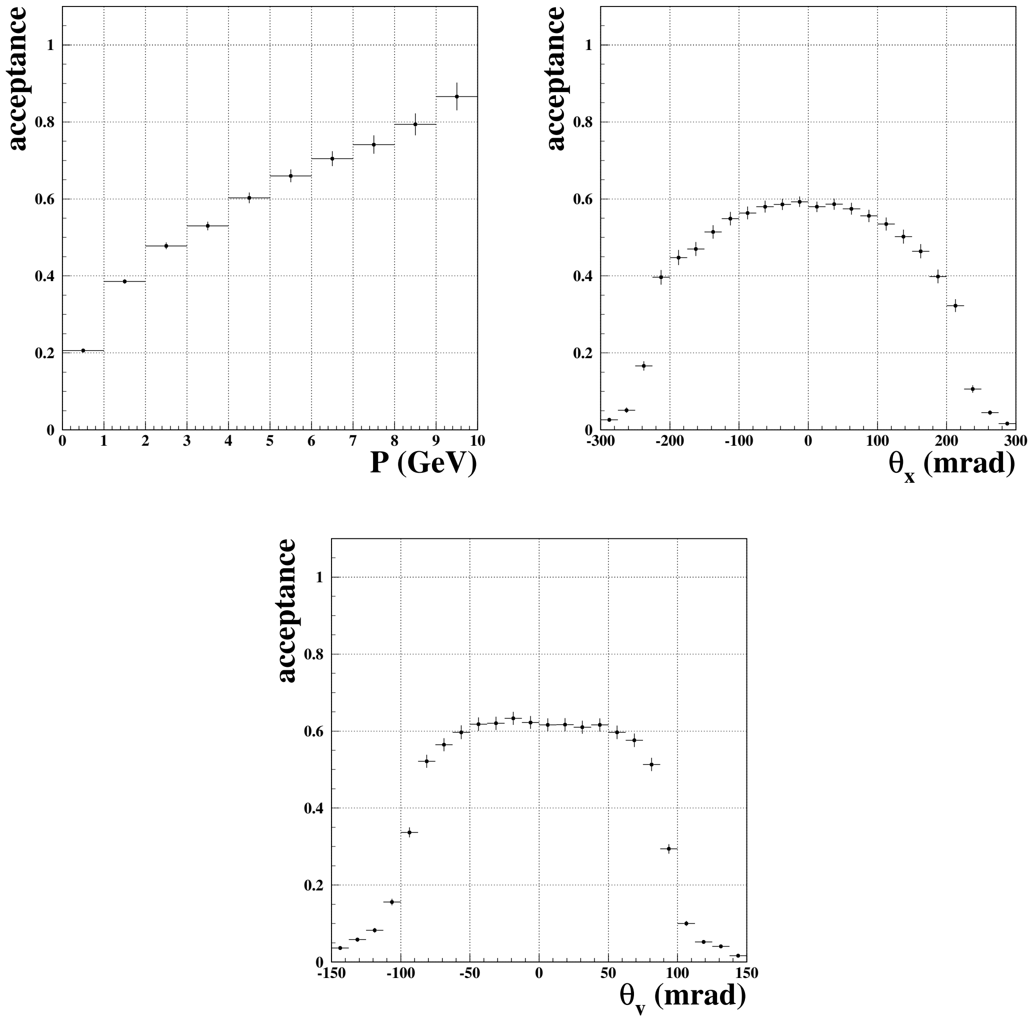

Figure 8: Acceptance for no cuts.

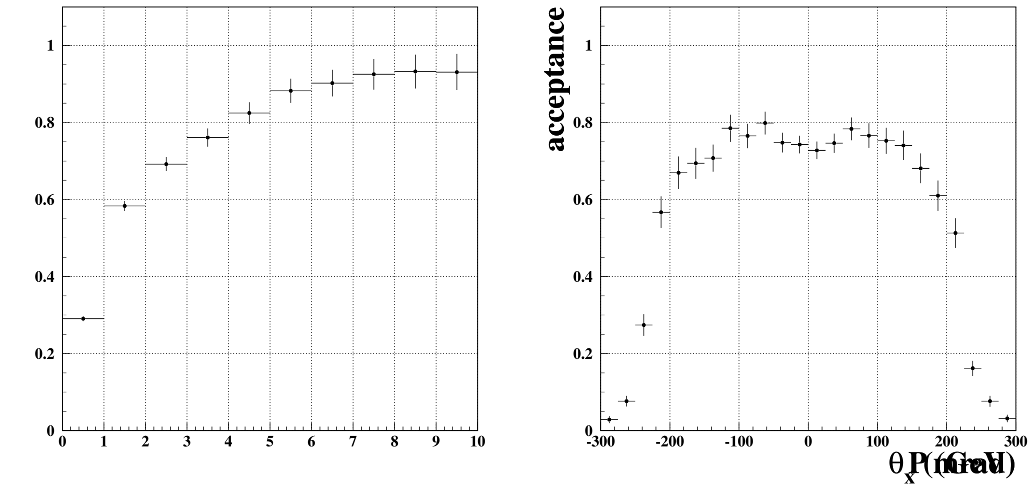

Figure 9: Acceptance for $|\theta_y| < 50mrad$

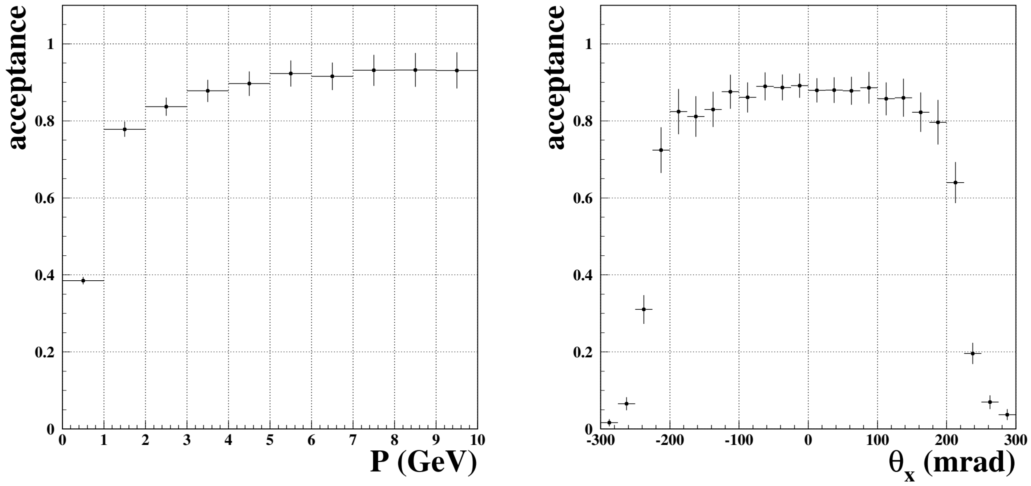

Figure 10: Acceptance in P for $|\theta_y| < 50mrad$, $|\theta_x| < 200mrad$. Acceptance in θ_x for $|\theta_y| < 50mrad$ and $P > 1GeV$

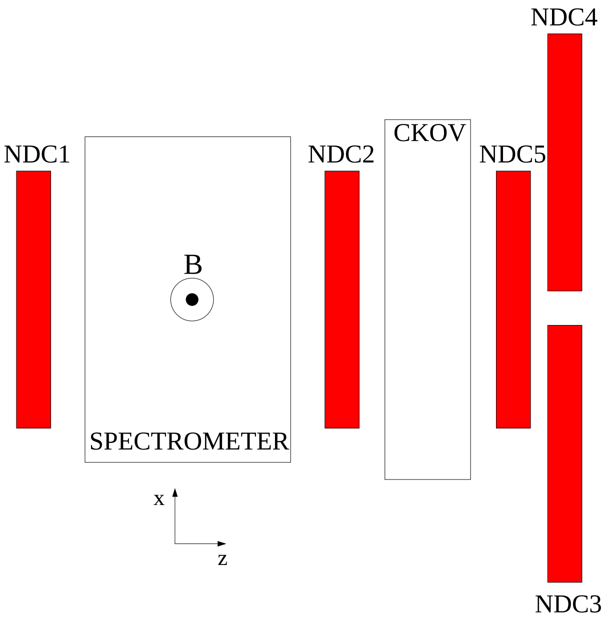

Figure 11: Schematic view of the relevant subdetectors for the NDC reconstruction.

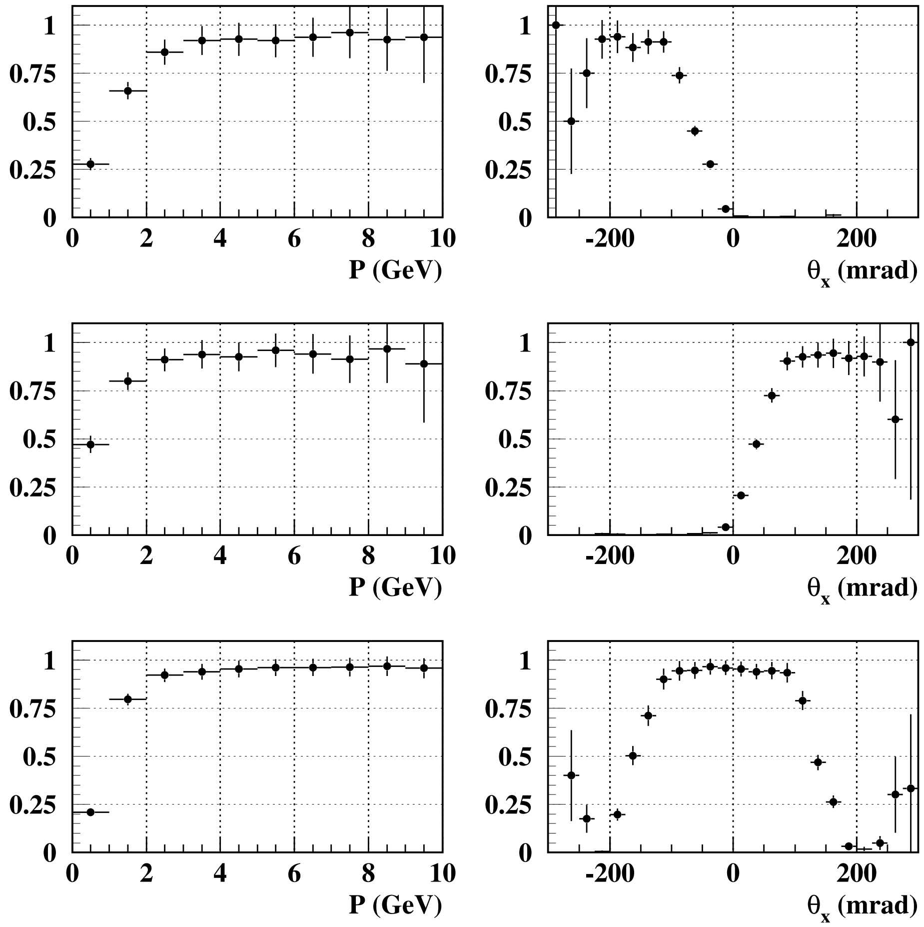

Figure 12: Acceptance of modules 3, 4 and 5 normalized to the acceptance of module 2, as function of p and θ_x

Lets assume, for simplicity that the only relevant modules for tracking are NDC1 (upstream the magnet), NDC2 (right downstream the magnet) and NDC5 (after CHE and before TOF). In addition, the thin target provides the Vertex Point, VP.

The procedure is valid if the probability of observing a hit (or a segment) in a given module, when a track crosses it, is independent from the probability of observing a hit (segment) in any other module for this same track. In principle this should be true, although one need to check that effects like saturation near the beam spot do not correlate the modules.

To compute efficiencies, the following samples of tracks are built for both real data (RD) and Monte Carlo data (MC). The samples are always built from thin target Al at 12.9 GeV.

In the following, "VP" means "use vertex point", "NDC1" means "use a $3D$ segment in module NDC1" and the same for all the other modules.

- Sample 1 (trk-i) built from VP + NDC2
- Sample 2 (trk-ii) built from VP + NDC5

5.3 Hit efficiency

Hit efficiency maps can be produced directly from thin target data

1. Use trk-i to compute hit efficiency map in NDC5 and NDC1
2. Use trk-ii to compute hit efficiency map in NDC2 and NDC1

For each case the hit efficiency is computed by extrapolating the track to the corresponding plane and searching whether there is a hit or not in a road around the track. This procedure allows to compute hit efficiency as a function of (p, θ_x, θ_y), thus we can measure the drop of efficiency associated to the saturation near the beam spot for NDC1. In fact, hit efficiency for NDC1 can be estimated independently using trk-i and trk-ii. Saturation effects should be negligible for NDC5. If they are also negligible for NDC2, the measurements using trk-i and trk-ii samples should yield equivalent results. Otherwise one can use trk-ii to estimate saturation effects bot in NDC1 and NDC2.

Hit efficiency should be independent of track momentum in the limit of single-track multiplicity (or sufficiently large opening angle between tracks) but track-to-track correlation may introduce a dependence with momentum, at least in NDC1. This must be checked.

Next we introduce hit efficiency in the MC. Using the technique outlined above,saturation effects should be correctly described.

5.4 Segment efficiency

Once hit efficiency maps have been produced and introduced in the MC it is possible to compute segment efficiency for both RD and MC, in exactly the same way as we have done for hit efficiency. The procedure is simply to count whether there is a segment in the module which has not been used to build the track. Comparison between RD and MC gives us directly corrections on segment efficiency in bins of p, θ_x, θ_y. As with the hit efficiency, segment efficiency may depend on p due to track-to-track correlations.

In fact, if the hit efficiency map is correct, then the MC should describe correctly segment efficiency in NDC2 and NDC5 where we expect negligible track-to-track correlations. Instead, the segment efficiency for NDC1 could reflect the effect of track-to-track correlations. This are hadronic model-dependent, and therefore the result obtained with the MC does not necesarily agree with the result obtained with data. However, data can be used to correct the MC calculation in bins of p, θ_x, θ_y.

5.5 Measurement of the momentum

The momentum of a given track is measured by means of the bending on the dipole magnet. The procedure is sketched here assuming that one has a $3D$ segment upstream and a $3D$ segment downstream the magnet. However, strictly speaking one only needs a segment downstream the magnet, since the procedure outlined below is identical if one has such segment and a $3D$ point upstream the magnet. Vertex constraint guarantees that such a point is always present.

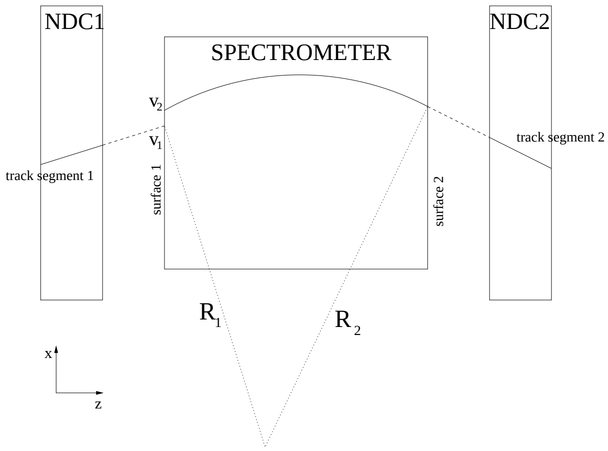

Figure 13: Matching through the spectrometer. v_1 is the state vector of track segment 1 extrapolated to the spectrometer entrance and v_2 the state vector of track segment 2 extrapolated to the spectrometer exit. The intersection of the normal to the track extrapolations in the bending plane defines the two radius R_1 and R_2. These should be comparable for track segments belonging to the same particle.

The first step is to associate the two segments by comparison in both the XZ (bending plane) and the YZ plane. A first matching χ^2 is defined through the quantity $\Delta R = R_1 - R_2$ (Fig. 13), assuming a homogeneous magnetic field: $\chi^2_R = (\Delta R^2/\sigma_{\Delta R})^2$. A second matching χ^2 is build using the y coordinate and its corresponding slope y' given the fact that the bending in the YZ projection is small. Assuming an average momentum, track segments in NDC1 and NDC2 are extrapolated to the same NDC1 surface to compute the quantity $\chi^2_y = (\Delta y \;\; \Delta y')(C_{\Delta y} + C_{\Delta y'})^{-1}(\Delta y \;\; \Delta y')^T$. The magnetic field inhomogeneities and the non zero bending in the YZ plane will introduce non negligible contributions to χ^2_R and χ^2_y respectively, which must be taken into account when applying cuts. In the case of a good matching, a first estimation of the momentum is done taken the weighted average of R_1 and R_2 as the radius of curvature R in the bending plane:

$$p_0 = \frac{0.3 \cdot |R| \cdot B_{avg}}{sin\alpha} \tag{2}$$

where α is the angle between the initial momentum and the magnetic field, and B_{avg} is the average magnetic field, which turns out to be 0.325 Tesla. The initial charge will be $q_0 = R/|R|$.

The second step consists in looping over momenta around p_0 to obtain a χ^2/ndf versus p distribution, which is fitted to a parabola. The momentum and its error are then computed using the equation of the parabola.

The momentum resolution as a function of the momentum achieved with this method is shown in Fig. 14. Notice the good agreement between RD and MC, which guarantees that MC can be used to unfold resolution effects.

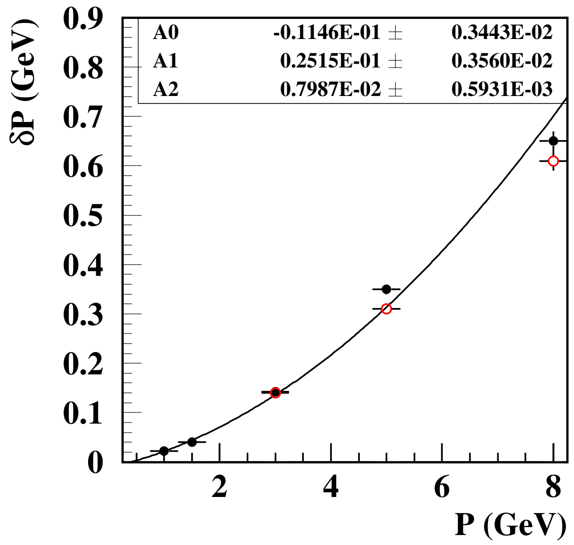

Figure 14: Momentum resolution for 1, 1.5, 3, 5 and 8 GeV/c no target monte carlo, and for 3, 5 and 8 GeV/c no target data. The curve represents the fit of the MC points to a parabola. The agreement between data and MC is excellent.

5.6 Track efficiency

To compute track efficiency we need to build tracks from segments and/or the VP. To measure the track momentum we need at leat VP and NDC2. Resolution improves (and fake-track background is reduced) if NDC1 is present. If NDC5 (NDC3, NDC4) is present, resolution improves and one has better matching with PID detectors.

If the track is built using VP and NDC2 the tracking efficiency is simply the segment efficiency for NDC2 multiplied by the matching efficiency NDC2-vetex, that is, the number of times that the NDC2 segment can be successfully extrapolated to the vertex reference plane and matched with a reasonable $\chi 2$ to the VP.

In fact, the matching NDC2-vertex matching $\chi 2$ can be computed from RD and MC. This quantity is not well reproduced by the MC, since the parameterization of the time-to-distance relationship in the Nomad drift chambers, does not fully acount for the dependence of the resolution with the track angle, among other effects. However, one can, as proposed for segment efficiency, use the data measurement to correct the MC.

Once the basic track (VP + NDC2) is built, one adds the NDC1 segment that better matches the track. Notice that there can be more than one segment in NDC1 (due to multiple tracks) or none (due, for example, to saturation). This later case is already taken into account in the segment efficiency. One can now compute (using RD and MC) the matching $\chi 2$ of the closest segment to the VP+NDC2 track extrapolated to NDC1, and add the segment if the $\chi 2$ is acceptable. The same procedure allows to add NDC5 (NDC3, NDC4). Eventually, one can recover some efficiency by searching for NDC1 matches on those NDC2 segments where one fails to find a VP match (and adding later VP extrapolating from NDC1, which is closer to the vertex) [1]. Ultimately, tracking efficiency must be computed in bins of p, θ_x, θ_y, and the MC tuned up so that it reproduces the RD.

[1] This procedure eliminates the need to use different track types. One uses always all the available information to build a track. Tracking efficiency should be close to the one previously found adding the three track types

5.7 tracking mini-dst

All the studies above have to be done from the minidst, or, if one wants to keep the mini-dst "mini", perhaps for a specially designed mini-dst. But the bottom line is that we should make it possible to carry them at "analysis level", that is, reading a bhep-like mdst (no Gaudi dependences, etc). Basically, this tracking mdst should have all the needed information for trk-i through trk-iv. Momentum, hits in each plane not included in the track within one or more roads, number of segments found in the module not included in the fit, chi2, and various extrapolations.

6 PID

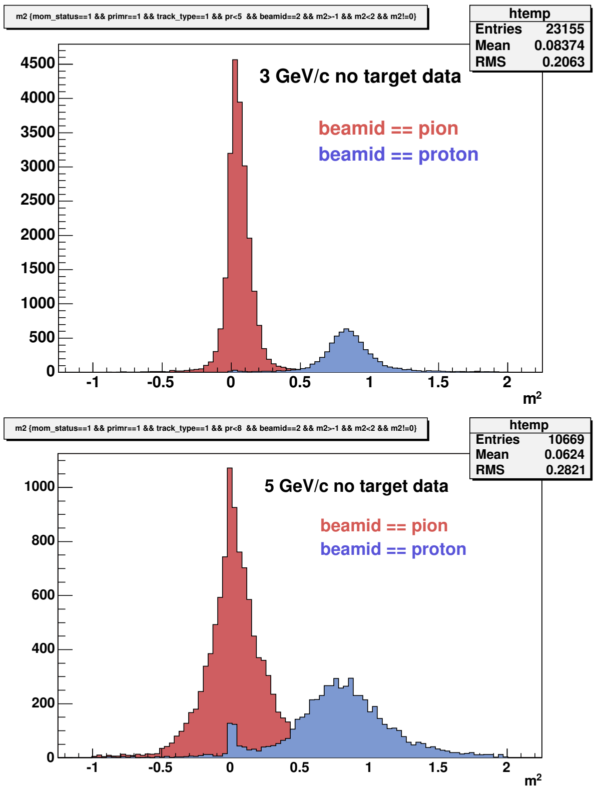

Figure 15: Mass squared as measured by the TOF system for 3 GeV/c empty target data (upper) and 5 GeV/c empty target data (bottom)

HARP forward spectrometer provides very good π/p and e/p separation. TOF alone provides a separation of better than 5 σ between protons and pions (Fig. 15) for $p <$ 3GeV/c, and can achieve good π/p separtion up to 5 GeV/c. Specifically, for beam particles of momentum 3 GeV/c, a cut on $m^2 < 0.5$ yields a pion efficiency of 94.1 % with a 98.6 % purity, while for beam particles of momentum 5 GeV/c, a cut on $m^2 < 0.4$ yields a pion efficiency of 88.6 % with a 91.9 % purity.

Conversely, above 4 GeV/c, π/p separation using CHE is good (Fig. 16). Thus one can achieve efficiencies of better than 90% with purity around 98 % in the full momentum range. e/π separation can rely on ECAL (Fig. 17), and, at low momentum, one can also use CHE information (CHE threshold is at 2.6 GeV/c where most of the electrons, arising from gamma conversions and secondary interactions are).

The fact that the pion momentum distribution peaks at 2 GeV/c (see Fig. 2) where one has essentially 100 % separation of pions from other species at high efficiency using TOF, makes PID very simple for this analysis.One simply needs to:

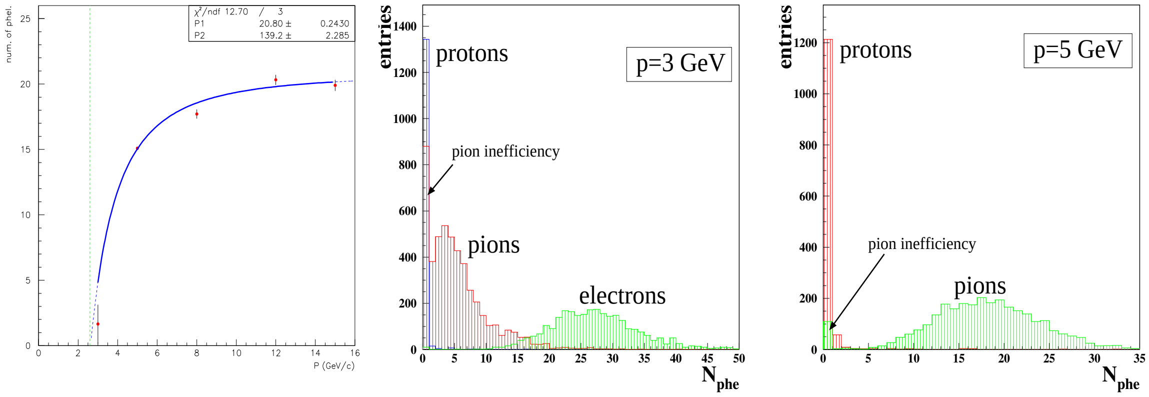

Figure 16: On the left, photoelectron yield as a function of momentum for a selected sample of pions. The experimental points are fitted to the theoretical curve $N_{phe} = N_0 \cdot [1 - (1 + (m/p)^2)/n^2]$, where n is the refraction index of the gas, m is the pion mass, p the momentum and N_0 the photoelectron yield in the saturation regime. The pion threshold is found to be at 2.6 GeV/c. Center and right, photoelectron yield for pions, electrons and protons at 3 and 5 GeV/c respectively. Pure samples are selected using the beam detectors.

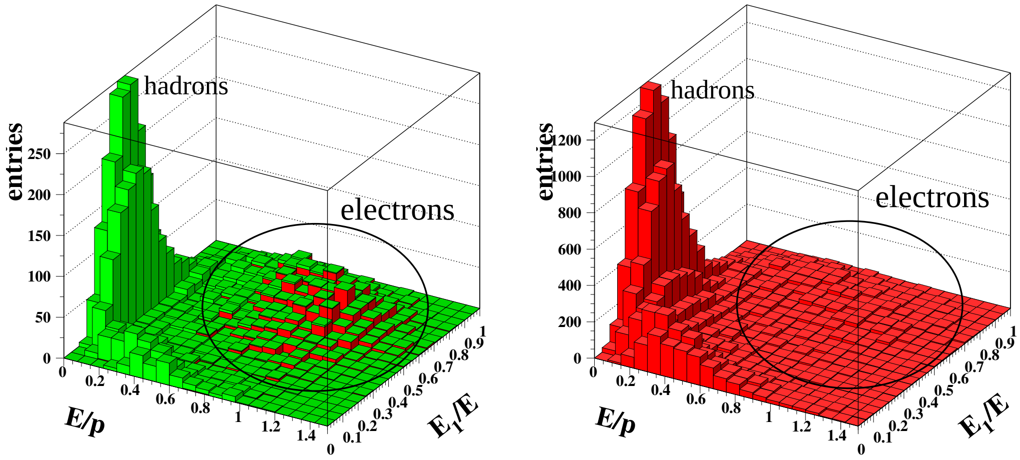

Figure 17: Particle yields as a function of E_1/E and E/p for 3 GeV/c no target (left) and 12.9 GeV/c Al thin target. (right). E is the total energy deposited in the calorimeter ($E_1 + E_2$).

1. Set a cut on $m^2 < 0.45$ 2 for $p < 4$ GeV/c.
2. Require a hit in CHE for $5 < p < 6$ GeV/c.
3. Beteen 4 and 5 GeV/c, one combines the two previous cuts.
4. Set an electron veto. No hit in CHE for $p < 2.6$ GeV/c (CHE pion threshold). For $p > 2.6$ GeV/c require the track consisten with not being an electron in ECAL (if ECAL matching available). Notice that electron background is small at high momentum. it is model dependent).

6.1 PID hit efficiency

Hit efficiency for the various PID detectors can be computed using data. One extrapolates the track to the detector reference surface and finds whether a hit can be found in a road around the track. The procedure should be straight forward and a map in bins of θ_x, θ_y can be produced for each relevant PID detector.

6.2 PID hit-track matching efficiency

Matching efficiency between tracks and PID hits will be affected by the same problem than segment-to-segment matching efficiency. The distributions will not be the same in data and in MC. However, also here we can compute the efficiency due to a given cut in matching $\chi 2$ from the data themselves.

7 Summary

The most challenging and time-consuming building blocks of HARP analysis (tracking algorithm, alignment, detector calibration, Monte Carlo simulation of detectors) have been completed. The current effort is focused on optimizing the Monte Carlo description of the detector, understanding tracking efficiency, defining optimal PID and complete the unfolding procedure.

The data processing needed for production of analysis DSTs will be completed by the end of the year (or early January) for both data (K2K thin target) and Monte Carlo. Preliminary results should be available in early February. Publication-quality results should be available in March.